

# Long-Term Preservation of Cones and Improvement in Visual Function Following Gene Therapy in a Mouse Model of Leber Congenital Amaurosis Caused by Guanylate Cyclase-1 Deficiency

Marija Mihelec, Rachael A. Pearson, Scott J. Robbie, Prateek K. Buch, Selina A. Azam, James W.B. Bainbridge, Alexander J. Smith, and Robin R. Ali

## Abstract

Leber congenital amaurosis (LCA) is a severe retinal dystrophy manifesting from early infancy as poor vision or blindness. Loss-of-function mutations in *GUCY2D* cause LCA1 and are one of the most common causes of LCA, accounting for 20% of all cases. Human *GUCY2D* and mouse *Gucy2e* genes encode guanylate cyclase-1 (GC1), which is responsible for restoring the dark state in photoreceptors after light exposure. The *Gucy2e*<sup>-/-</sup> mouse shows partially diminished rod function, but an absence of cone function before degeneration. Although the cones appear morphologically normal, they exhibit mislocalization of proteins involved in phototransduction. In this study we tested the efficacy of an rAAV2/8 vector containing the human rhodopsin kinase promoter and the human *GUCY2D* gene. Following subretinal delivery of the vector in *Gucy2e*<sup>-/-</sup> mice, GC1 protein was detected in the rod and cone outer segments, and in transduced areas of retina cone transducin was appropriately localized to cone outer segments. Moreover, we observed a dose-dependent restoration of rod and cone function and an improvement in visual behavior of the treated mice. Most importantly, cone preservation was observed in transduced areas up to 6 months post injection. To date, this is the most effective rescue of the *Gucy2e*<sup>-/-</sup> mouse model of LCA and we propose that a vector, similar to the one used in this study, could be suitable for use in a clinical trial of gene therapy for LCA1.

## Introduction

**L**EBER CONGENITAL AMAUROSIS (LCA) is a genetically heterogeneous autosomal recessive disorder causing severe retinal degeneration (den Hollander *et al.*, 2008). It is generally diagnosed in early infancy and is characterized by poor vision or blindness with nystagmus and dramatically reduced or absent electroretinogram. LCA1 is caused by mutations in the *GUCY2D* gene and is the most prevalent form of LCA, accounting for up to 20% of all LCA cases (Hanein *et al.*, 2004; Hunt *et al.*, 2010).

Human *GUCY2D* and mouse *Gucy2e* genes encode the retinal guanylate cyclase-1 (GC1) protein, which is located in disc membranes of photoreceptor outer segments. The role of GC1 is to replenish cGMP levels after light exposure (reviewed in Koch *et al.*, 2002). In the dark, cGMP levels are sustained at a steady rate, keeping the cGMP-gated channels open and maintaining partial depolarization of the cells by

allowing influx of the inward current. Exposure to light leads to cGMP hydrolysis and channel closure, facilitating a sharp decline in intracellular Ca<sup>2+</sup> and hyperpolarization of the cells. Under low Ca<sup>2+</sup> concentrations, guanylate cyclase-activating proteins (GCAPs) stimulate GC1 activity resulting in cGMP synthesis, reopening of the channels, and dark state restoration. Mutations that inactivate GC1 lead to inability to produce cGMP, persistent closure of the cGMP-gated channels, and therefore a state equivalent to constant light exposure (Larhammar *et al.*, 2009; Hunt *et al.*, 2010).

The phenotype of the *Gucy2e*<sup>-/-</sup> mouse differs from that of patients with LCA1 regarding rod function. Patients with LCA1 have no detectable rod function as measured by electroretinography (ERG), whereas *Gucy2e*<sup>-/-</sup> mice exhibit diminished, but persistent rod function. This results from functional redundancy provided by the GC2 gene expressed in mouse rods, although why this mechanism appears not to be operating in humans is unclear (Baehr *et al.*, 2007; Helten

*et al.*, 2007). In both mouse and human, cone function is absent from birth. Cone degeneration in the mouse is detectable from 9 weeks of age and continues over the next 6 months (Coleman *et al.*, 2004). It has been shown that, despite poor rod function, the retina of patients with LCA1 may still be largely intact in patients ranging from 20 to 53 years of age (Pasadhika *et al.*, 2010). LCA1 may therefore be more amenable to gene therapy than other forms of LCA in which photoreceptor cell survival is compromised much earlier.

Gene therapy for LCA1 has previously been evaluated in the GUCY1\*B chicken (Williams *et al.*, 2006) and *Gucy2e*<sup>-/-</sup> mouse (Haire *et al.*, 2006; Boye *et al.*, 2010). The initial studies, using a bovine GC1 transgene and either a lentiviral vector (Williams *et al.*, 2006) or rAAV2/5 vector (recombinant adeno-associated virus type 2 [AAV2] vector pseudotyped with AAV5 capsid) (Haire *et al.*, 2006) resulted in short-term improvement of retinal function in the GUCY1\*B chicken, but no improvement in the *Gucy2e*<sup>-/-</sup> mouse. The more recent study, using rAAV2/5 and a mouse transgene, achieved significant restoration of visual function in the *Gucy2e*<sup>-/-</sup> mouse (Boye *et al.*, 2010). In treated *Gucy2e*<sup>-/-</sup> eyes, cone-mediated (photopic) b-wave amplitudes increased up to 45% of wild-type levels, and cones were preserved for up to 3 months posttreatment. Furthermore, behavioral analyses demonstrated improvement in visual acuity and contrast sensitivity. No improvement in rod function was reported.

In this study, we assessed the long-term efficacy of rAAV2/8-mediated transfer of a human GC1 transgene and have achieved the most effective rescue of the *Gucy2e*<sup>-/-</sup> mouse model of LCA to date.

## Materials and Methods

### Experimental animals

*Gucy2e*<sup>-/-</sup> animals were provided by D.L. Garbers (Dallas, TX). The homozygous line was maintained on a mixed 129/SvJ and C57BL/6J background. To determine whether any improvements following gene therapy fell within the normal range for wild-type animals, pure inbred C57BL6/J were used as wild-type controls. All the experiments were approved by the University College London (London, UK) Ethics Committee and were performed under U.K. Home Office license. The procedures were conducted in accordance with the Association for Research in Vision and Ophthalmology (Rockville, MD) *Statement for the Use of Animals in Ophthalmic and Vision Research*.

### Plasmid construction and production of rAAV2/8

Human GUCY2D and mouse *Gucy2e* cDNAs were cloned into the pD10\_hRK\_GFP construct (Khani *et al.*, 2007). Before cDNA insertion, the gene encoding green fluorescent protein (GFP) was removed and cDNA was inserted in between the human rhodopsin kinase (hRK) promoter and the simian virus 40 (SV40) polyadenylation site to form the following constructs: pD10\_hRK\_hGUCY2D (total length, 8162 bp) and pD10\_hRK\_m*Gucy2e* (total length, 7979 bp). The constructs were verified by sequencing.

Recombinant AAV2/8 was produced by a previously described tripartite transfection method (Gao *et al.*, 2002) into 293 cells. AAV8 packaging, helper, and pD10\_hRK\_hGUCY2D or pD10\_hRK\_m*Gucy2e* plasmids were combined with

polyethylenimine (PEI; Polysciences, Eppelheim, Germany) and left to form complexes for 10 min. The mixture was added to HEK293 cells and left for 24 hr. The cells were harvested and concentrated 2 days after transfection, and lysed using repeated freeze-thaw cycles to release the vector. The HEK293 cell nucleic acid component was removed by Benzonase (Sigma-Aldrich, Dorset, UK) treatment and virus preparation was cleared of cellular debris by multiple centrifugation steps, followed by previously described purification by ion-exchange chromatography (Davidoff *et al.*, 2004). The virus preparation was concentrated in a Vivaspinn 4 concentrator (10 kDa; Sartorius Stedim Biotech/Fisher Scientific, Loughborough, UK), washed in phosphate-buffered saline (PBS), and concentrated further to 100–150  $\mu$ l. Viral particle titers were determined by dot-blot analysis of purified virus preparations and plasmid controls of known concentrations.

### Subretinal injections

Subretinal injections of viral vectors were performed on postnatal day 10 (P10) in the right eyes of *Gucy2e*<sup>-/-</sup> mice. Left eyes were left as untreated internal controls. Double injections of 1.5  $\mu$ l each were performed per eye, targeting superior and inferior hemispheres of the retina. The technique used to deliver subretinal injections was previously described (Tan *et al.*, 2009).

### Electroretinographic analysis

Electroretinograms (ERGs) were recorded from both eyes of injected *Gucy2e*<sup>-/-</sup> mice and age-matched C57BL6/J wild-type controls starting from 2 weeks post injection. ERGs were subsequently recorded on a 2-weekly basis up to week 8, and then monthly up to 6 months post treatment when the animals were sacrificed. Uninjected left eyes of treated animals were regarded as untreated controls. All animals were dark adapted overnight before ERG recordings. The animals were anesthetized with a single intraperitoneal injection of a 0.01-ml/g mixture of Domitor (1 mg/ml medetomidine hydrochloride), ketamine (100 mg/ml), and water at a ratio of 5:3:42 before recording. The pupils were dilated with a drop of Minims Tropicamide 1% (Bausch & Lomb/Chauvin Pharmaceuticals, Essex, UK). Midline subdermal ground and mouth reference electrodes were first placed, followed by eye electrodes that were allowed to lightly touch the corneas. A drop of Viscotears 0.2% liquid gel (Dr. Robert Winzer Pharma/OPD Laboratories, Watford, UK) was placed on top of the electrodes to keep the corneas moistened during recordings. ERGs were recorded with commercially available equipment (Espion E2; Diagnosys, Lowell, MA). Bandpass filter cutoff frequencies were 0.312 Hz (low-frequency cutoff) and 1000 Hz (high-frequency cutoff). Scotopic, rod-mediated responses were obtained from dark-adapted animals at the following increasing light intensities: 0.001, 0.01, 0.1, 1, 3, 5, and 10 cd/m<sup>2</sup>. Ten responses per intensity were recorded for the first three intensities with 10-sec dark adaptation between each. Five responses were recorded for all the subsequent steps with 30-sec dark adaptation between each. Responses were averaged for each intensity. For the rod-mediated b-wave responses amplitudes were analyzed at a scotopic light intensity of 0.01 cd/m<sup>2</sup>.

Photopic, cone-mediated responses were performed after a 10-min light adaptation on a background light intensity of 20 cd, which was used as background intensity for the duration of photopic recordings, flash and flicker. Recordings were obtained at the following increasing light intensities: 0.1, 1, 3, 5, 10, and 20 cd/m<sup>2</sup>. Twenty-five responses were averaged for each intensity, with a 60-sec light adaptation interval between each step. For the cone-mediated b-wave responses amplitudes were analyzed at a photopic light intensity of 20 cd/m<sup>2</sup>.

Photopic flicker followed photopic flash recordings, and consisted of 25 flashes per frequency at the following frequencies: 0.5, 2, 5, 10, 15, and 30 Hz.

### Optomotor testing

Contrast sensitivities and visual acuities of treated and untreated eyes were measured by observing the optomotor responses of mice to rotating sinusoidal gratings (OptoMotry®; CerebralMechanics, www.cerebralmechanics.com/CerebralMechanics\_Inc./OptoMotry.html). Mice reflexively respond to rotating vertical gratings by moving their head in the direction of grating rotation. The protocol used yields independent measures of the acuities of right and left eyes, based on the unequal sensitivities of the two eyes to pattern rotation: right and left eyes are most sensitive to counter-clockwise and clockwise rotations, respectively (Douglas *et al.*, 2005; Alexander *et al.*, 2007). *Gucy2e*<sup>-/-</sup> mice were previously described to have normal optomotor rod behavior (Boye *et al.*, 2010). Therefore, to exclude any rod input, mice were light adapted for at least 30 min before testing. A double-blind two-alternative forced choice procedure was employed, in which the observer was blinded to both the direction of pattern rotation and to which eye received treatment. Acuity was defined as the highest spatial frequency (at 100% contrast) yielding a threshold response, and contrast sensitivity was defined as 100 divided by the lowest percent contrast yielding a threshold response. For photopic acuity, the initial stimulus was a 0.200 cycles/degree sinusoidal pattern with a fixed 100% contrast. For photopic contrast sensitivity measurements, the initial pattern was presented at 100% contrast, with a fixed spatial frequency of 0.128 cycles/degree. Visual acuity and contrast sensitivity were measured under photopic conditions (62 log cd m<sup>-2</sup>). Visual acuities and contrast sensitivities were measured for both eyes of each mouse at least four times on independent days. Data for naive *Gucy2e*<sup>-/-</sup> mice are presented alongside for comparison (animals 1 and 2).

### Tissue preparation for immunohistochemistry and crude membrane protein preparation

All animals treated with low-titer vector were taken for immunohistochemistry. For immunohistochemistry performed on dark-adapted eyes, the animals were dark adapted overnight and sacrificed in the dark, with the red light head torch as the only light source. For those eyes collected in the light a cautery mark was placed on the superior limbus to aid in orientation. The cornea was pierced and the eye placed in 4% paraformaldehyde (PFA) at 4°C overnight. Corneas were removed and a small V-shaped mark was cut out of the sclera, where the cautery mark was present. Lenses were removed and eyecups placed in a 20% sucrose-PBS solution until sunken. The eyecups were then embedded in

optimal cutting temperature (OCT) embedding medium (Raymond A. Lamb/Thermo Fisher Scientific, East Sussex, UK), and frozen in isopentane previously cooled in liquid nitrogen. Embedded eyes were kept at -80°C until sectioned.

For Western blotting, a crude membrane preparation was used to extract protein from the snap-frozen retinas. Each retina was placed in 100 µl of low-salt homogenization buffer (10 mM morpholinepropanesulfonic acid [MOPS], 5 mM mercaptoethanol in water, and protease inhibitors added). Tissue was broken up by multiple passages through a 25-gauge needle. Salt content was then raised to 0.25 M by adding 5 M NaCl and the homogenate was centrifuged at 4°C for 5 min at 900×g to remove large debris. The extract was further centrifuged at 15,000×g for 30 min at 4°C, after which membrane pellets were resuspended in 50 µl of the low-salt homogenization buffer.

### Immunohistochemistry

Immunofluorescence for GC1, cone arrestin, and  $\alpha$ -transducin was performed on freshly cut, frozen retinal sections (thickness, 18 µm). Slides were incubated in blocking buffer (2% normal goat serum [Dako, Ely, UK], 1% bovine serum albumin [BSA], 0.1% Triton X-100 in PBS) for 1 hr at room temperature. Antibodies were diluted and added to their respective slides at the following dilutions: polyclonal rabbit anti-GC1, 1:1000 (GC1 antibody used for immunohistochemistry was generously provided by A. Dizhoor, Salus University, Elkins Park, PA); polyclonal rabbit anti-cone arrestin, 1:10,000 (Millipore, Watford, UK); and polyclonal rabbit anti-cone  $\alpha$ -transducin, 1:2000 (Santa Cruz Biotechnology, Santa Cruz, CA), and left to incubate at 4°C overnight. Slides were thoroughly washed in PBS and the following secondary antibodies were diluted in block solution and applied: for GC1 and cone arrestin, Alexa Fluor 488 goat anti-rabbit IgG conjugate was used (diluted 1:2500; Molecular Probes, Paisley, UK), and for  $\alpha$ -transducin Alexa Fluor 594 donkey anti-rabbit IgG conjugate was used (diluted 1:1000; Molecular Probes). Slides were incubated with secondary antibodies for 2 hr at room temperature, followed by PBS washes. Hoechst (Sigma-Aldrich) nuclear counterstain was used diluted to 1 µg/ml in PBS. Slides were mounted in fluorescent mounting medium (Fluormount; Dako) and staining was analyzed by microscopy (Leica TCS SPE confocal microscope; Leica, Mannheim, Germany).

### Western blotting

Membrane protein extracts were quantified in a Bio-Rad protein assay (Bio-Rad, Hemel Hempstead, UK). Equal concentrations of each sample were left at 37°C for 30 min before 10× sample buffer was added. The samples were then loaded onto 6% polyacrylamide gels and, after gel electrophoresis, transferred to nitrocellulose membrane for Western blotting. After blocking the membrane in block solution (5% skimmed milk powder-1% bovine serum albumin [BSA; Sigma-Aldrich]-0.05% Tween 20 in PBS) overnight at 4°C, goat polyclonal anti-GC1 antibody [diluted 1:250; ROS-GC1 (C-13), Santa Cruz Biotechnology] was added and left at room temperature for 2 hr. Membrane was thoroughly washed in PBS-0.05% Tween 20 and incubated with a horseradish peroxidase (HRP)-conjugated rabbit anti-goat IgG antibody (diluted 1:5000; Dako) in block solution for 1 hr at

room temperature. After PBS–0.05% Tween 20 washes, signal was developed with Amersham enhanced chemiluminescence (ECL) Plus Western blotting detection reagents (GE Healthcare, Chalfont St Giles, UK). Subsequent to image analysis, the membrane was stripped of antibodies, using prewarmed stripping buffer (100 mM mercaptoethanol, 2% sodium dodecyl sulfate [SDS], 62.5 mM Tris-HCl), and the stripping procedure was verified by repeating the signal detection process followed by thorough washes in PBS–0.05% Tween 20. The membrane was reblocked with the same blocking solution as described previously and mouse monoclonal anti-Kv2.1 potassium channel protein antibody (diluted 1:10,000; UC Davis/NIH NeuroMab facility, Davis, CA) was added and left at 4°C overnight. The next morning the membrane was washed thoroughly in PBS–0.05% Tween 20 and incubated with an HRP-conjugated anti-mouse IgG antibody diluted 1:10,000 in block solution for 1 hr at room temperature. Signal detection was repeated as described previously.

#### Real-time RT-PCR

RNA was extracted from retinas treated with the high-titer vector at 5 months post injection. The numbers for all real-time RT-PCR analyses were as follows: treated group,  $n=6$  eyes; untreated group,  $n=5$  eyes; C57BL/6J wild-type group,  $n=3$  eyes. RNA was extracted with an RNeasy mini kit (Qiagen, Crawley UK). Equal quantities and up to 1  $\mu$ g of RNA were used as a template for cDNA manufacture for each sample. cDNA was produced with a QuantiTect reverse transcriptase kit (Qiagen). Real-time quantitative RT-PCR (qRT-PCR) was performed with a commercial thermal cycler (7900HT; Applied Biosciences, Foster City, CA). All reagents were obtained from Roche Diagnostics (Burgess Hill, UK). The technique was based on FAM-labeled hydrolysis probes (Roche Diagnostics), and primers were designed for specific probe-binding regions using the Roche Universal Probe Library. The primers used to detect endogenous mouse *Gucy2e* were as follows: CATGGACCTCACCTTTGACC (forward) and CTGTGCGTTCTCGGATCA (reverse) in combination with Roche universal probe #67. To detect the introduced human *GUCY2D* transcript the following primers were used: CGGCTGCTTACACAGATGC (forward) and GTACTCGGGCTCCACTGGT (reverse) in combination with Roche universal probe #5. To measure cone arrestin levels, the following primers were used: TGTGTTTGTTCAGGAGTTCA CA (forward) and AGGCCCTGCTTCTGACAGT (reverse) in combination with Roche universal probe #71. Cycling conditions for the endogenous mouse *Gucy2e* and cone arrestin reactions were 40 cycles of 94°C for 30 sec, 60°C for 1 min; and for the human *GUCY2D* transcript 40 cycles of 94°C for 30 sec, 50°C for 1 min. All reactions were performed in duplicate or triplicate. Absolute mRNA amounts were calculated on the basis of the standard curve of control DNA sample dilutions of known concentration, which was included for every PCR performed. Water control was also included for every primer–probe combination.

#### Statistical analyses

To analyze qRT-PCR, optometry, and cone quantification data, one-way analysis of variance (ANOVA) was used with Tukey's multiple comparison post-tests. Two-way ANOVA

for repetitive measures with Bonferroni post-tests was used to statistically evaluate ERG data. The Student *t* test was used to evaluate cone arrestin as a marker of cone numbers. All statistical analyses were performed with GraphPad Prism version 5.01 for Windows (GraphPad Software, San Diego, CA).

## Results

### *GC1 protein localization and levels in eyes of *Gucy2e*<sup>−/−</sup> mice following subretinal injections of AAV2/8 vector carrying a *GUCY2D* transgene*

Human *GUCY2D* cDNA was cloned into the AAV2 plasmid backbone with an hRK promoter and SV40 polyadenylation site. We have previously shown that this rhodopsin kinase promoter mediates efficient transgene expression in both rods and cones (Khani *et al.*, 2007; Pawlyk *et al.*, 2010; Sun *et al.*, 2010). The plasmid was packaged with AAV8 capsids to generate a recombinant AAV2/8 vector (rAAV2/8\_hRK\_hGUCY2D), using a tripartite transfection method in HEK293 cells, and purified by ion-exchange chromatography (Gao *et al.*, 2002). *Gucy2e*<sup>−/−</sup> mice were treated with two injections of 1.5  $\mu$ l of vector at  $7 \times 10^{11}$  vector genomes (VG)/ml (low titer) or  $4 \times 10^{12}$  VG/ml (high titer).

GC1 is localized to outer segments of mouse photoreceptors (Fig. 1a). Following subretinal injections of rAAV2/8\_hRK\_hGUCY2D in postnatal day 10 (P10) *Gucy2e*<sup>−/−</sup> mice, abundant GC1 was detected exclusively in photoreceptor outer segments for up to 6 months post treatment (latest time point examined; Fig. 1b), whereas no GC1 staining was observed in the untreated eyes (Fig. 1c). Western blot analysis confirmed that the transgene product was of the correct size at 120 kDa (Fig. 1d). We also examined, using real-time RT-PCR, the levels of *GUCY2D* transcript produced in *Gucy2e*<sup>−/−</sup> eyes 5 months after injection of high-titer rAAV2/8\_hRK\_hGUCY2D (Fig. 2). Total RNA was extracted from six treated retinas, as well as from the retinas of four untreated mice and three C57BL/6J wild-type controls. The human *GUCY2D* transcript levels in *Gucy2e*<sup>−/−</sup> eyes that had received high-titer vector were on average 30-fold higher than endogenous transcript levels in C57BL/6J wild-type retinas ( $p < 0.01$ , one-way ANOVA). However, as the transgene transcript lacks the natural 5' untranslated region (UTR), it may not be translated with the same efficiency as the endogenous mRNA. These results are consistent with our immunohistochemical staining (Fig. 1a–c), but not our Western blot data (Fig. 1d), which suggests that *Gucy2e*<sup>−/−</sup> mice that received either low- or high-titer vector have lower levels of GC1 compared with wild-type C57BL/6J mice. The inconsistency between the immunohistochemistry, qPCR, and immunoblot data might be explained by the use of two different antibodies for Western blotting and immunohistochemistry. However, it is not appropriate to use immunoblotting or immunohistochemistry as a way of comparing the levels of GC1 in treated *Gucy2e*<sup>−/−</sup> mice and untreated wild-type mice because the polyclonal antibodies used are raised against human GC1 and so most likely bind the human transgene product more efficiently than endogenous mouse GC1. It is therefore not possible to determine the levels of transgene product relative to endogenous protein in wild-type mice.

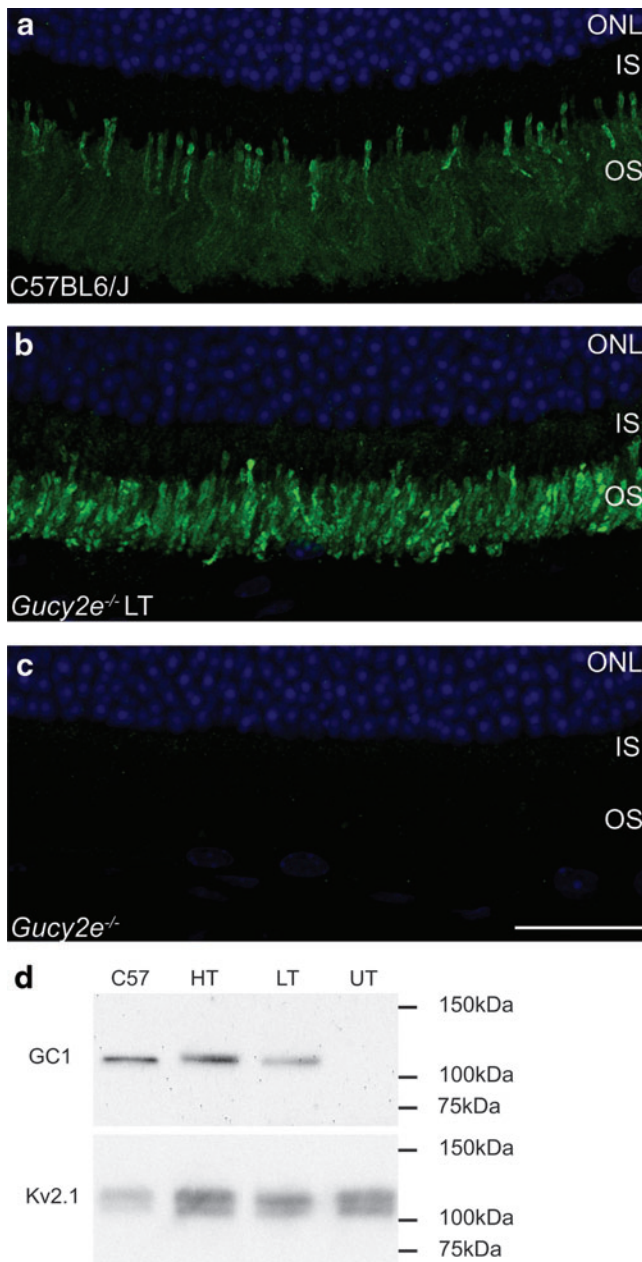


**FIG. 1.** Correct size and localization of guanylate cyclase-1 (GC1) protein in treated *Gucy2e*<sup>-/-</sup> eyes. GC1 immunofluorescence (green) was detected in the outer segments of photoreceptor cells in (a) wild-type eyes and (b) *Gucy2e*<sup>-/-</sup> eyes treated with low-titer (LT) vector. (c) No staining was observed in untreated *Gucy2e*<sup>-/-</sup> eyes. 4',6-Diamidino-2-phenylindole (DAPI) nuclear counterstaining is shown in blue. (d) Western blot showing 120-kDa GC1 protein in *Gucy2e*<sup>-/-</sup> eyes treated with low-titer (LT) or high-titer (HT) vector and in C57BL/6J wild-type controls, but not in *Gucy2e*<sup>-/-</sup> untreated eyes (UT). Kv2.1 was used as a loading control. OS, outer segments; IS, inner segments; ONL, outer nuclear layer. Scale bar: 25  $\mu$ m. Color images available online at [www.liebertonline.com/hum](http://www.liebertonline.com/hum)

#### Restored localization and increased levels of cone $\alpha$ -transducin in treated retinas

To modulate the sensitivity of the photoresponse and also to protect photoreceptors in bright light, key components of

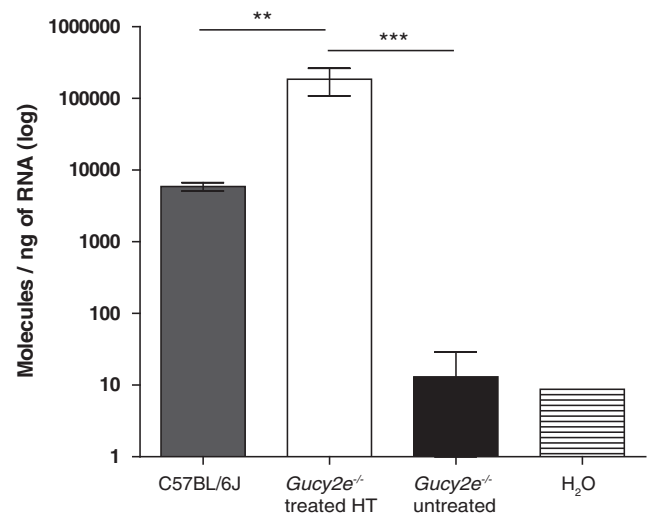


**FIG. 2.** *GUCY2D* transcript levels in *Gucy2e*<sup>-/-</sup> eyes treated with high-titer vector. Real-time RT-PCR analyses comparing levels of *GUCY2D* transcript in high-titer vector-treated *Gucy2e*<sup>-/-</sup> eyes with endogenous *Gucy2e* transcript in C57BL/6J wild-type eyes and untreated *Gucy2e*<sup>-/-</sup> eyes. The levels of introduced *GUCY2D* transcript in treated eyes are 30-fold higher than those seen in C57BL/6J wild-type control eyes ( $p < 0.01$ , one-way ANOVA). Transcript levels detected in untreated controls are significantly lower than the levels of *GUCY2D* transcript detected in treated *Gucy2e*<sup>-/-</sup> eyes ( $p < 0.001$ , one-way ANOVA).

the phototransduction cascade, including arrestin and the G-protein transducin, translocate between photoreceptor compartments in mouse rods and cones (Elias *et al.*, 2004; Lobanova *et al.*, 2010). In dark-adapted rods, arrestin is dispersed throughout the cell and translocates to the outer segments on exposure to light; the reverse is true for transducin. In cones, arrestin translocates in the same manner as in rods (Elias *et al.*, 2004). However, cone  $\alpha$ -transducin translocation is triggered only by high light intensities and the cones need to be saturated and unresponsive for a prolonged period of time (Lobanova *et al.*, 2010). It has been demonstrated previously that localization of cone  $\alpha$ -transducin is perturbed in *Gucy2e*<sup>-/-</sup> cone photoreceptors, with  $\alpha$ -transducin localized to the inner segments and synaptic regions of cones (Coleman and Semple-Rowland, 2005). Our results are consistent with these findings; we observed weak and mislocalized cone  $\alpha$ -transducin staining in untreated *Gucy2e*<sup>-/-</sup> eyes. In the treated eyes, however, immunohistochemical staining revealed increased levels of cone  $\alpha$ -transducin, correctly localized to the cone outer segments (Fig. 3a). It has also been reported previously that localization of cone arrestin is perturbed in *Gucy2e*<sup>-/-</sup> cone photoreceptors (Coleman and Semple-Rowland, 2005), and that cone arrestin remains in the outer segments and synaptic terminals regardless of light conditions. However, we did not observe a major difference in cone arrestin staining in C57BL/6J wild-type and untreated *Gucy2e*<sup>-/-</sup> mice (Fig. 3b). Although there was faint immunostaining throughout *Gucy2e*<sup>-/-</sup> cones that was not seen in wild-type cones, in light-adapted animals the bulk of the signal, as in wild-type animals, was present in cone outer segments and synaptic terminals. Furthermore, after dark adaptation, arrestin translocated normally throughout

cone photoreceptor cells. The localization and translocation of cone arrestin was not altered after administration of vector (Fig. 3b).

*Dose-dependent, long-term restoration of photoreceptor function in  $Gucy2e^{-/-}$  mice*

The effect of treatment on photoreceptor function was tested over a 6-month period by electroretinography (ERG).

ERGs were performed on treated and untreated  $Gucy2e^{-/-}$  mice and on age-matched C57BL/6J wild-type control animals. The average scotopic (rod-mediated) b-wave amplitude of untreated  $Gucy2e^{-/-}$  mice was approximately 35% of that of C57BL/6J wild-type animals at all time points examined. There was no significant difference in scotopic b-wave amplitudes after injection of control rAAV2/8\_hRK\_hrGFP or low-titer vector (data not shown). Scotopic b-wave amplitudes in  $Gucy2e^{-/-}$  mice treated with high-titer vector were, over time, significantly higher than those of untreated mice ( $p=0.0005$ , two-way ANOVA). The b-wave amplitudes were restored to 65–100% of wild type (Fig. 4a and b).

Restoration of cone function was achieved with both high- and low-titer vector (Fig. 4c). After injection of low-titer vector, cone-mediated b-wave amplitudes were on average 20% of that from wild-type mice and were significantly different from those of untreated  $Gucy2e^{-/-}$  mice at all time points examined ( $p<0.05$ , two-way ANOVA). In animals treated with high-titer vector, cone-mediated b-wave amplitudes were improved even further—on average 65% of wild type. Cone-mediated b-wave amplitudes from treated animals were significantly greater than those from untreated controls at each time point examined ( $p<0.001$ , two-way ANOVA). The cone-mediated ERG after injection of control rAAV2/8\_hRK\_hrGFP vector was not different from untreated controls (data not shown).

After subretinal injection of high-titer rAAV2/8\_hRK\_mGucy2e (vector carrying the mouse  $Gucy2e$  transgene) we observed an increase in scotopic and photopic b-wave amplitudes that was not significantly different from that achieved after administration of high-titer rAAV2/8\_hRK\_hGUCY2D ( $p>0.05$ , two-way ANOVA; Fig. 5a and b). This similarity in the efficacy of the two vectors probably reflects the 87% homology between mouse and human GC1 proteins.

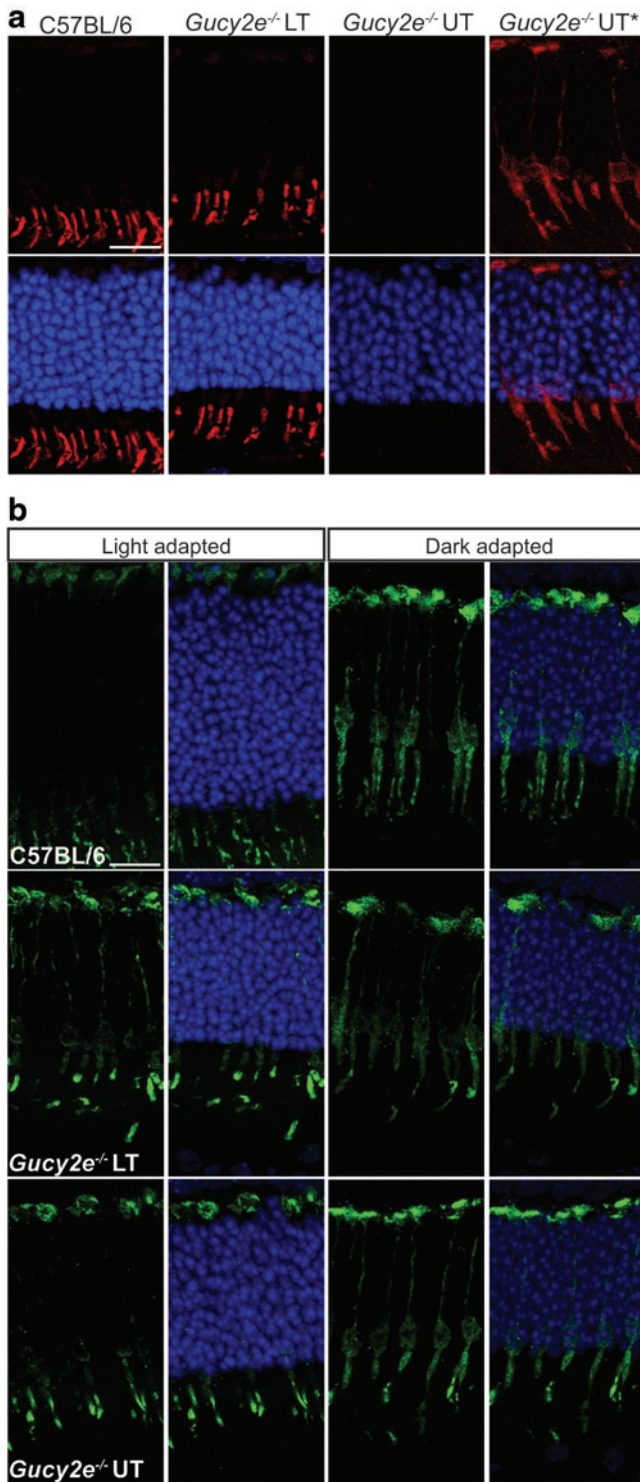


**FIG. 3.** Cone  $\alpha$ -transducin levels and localization are restored in  $Gucy2e^{-/-}$  treated eyes. C57BL/6J wild-type,  $Gucy2e^{-/-}$  eyes treated with low-titer (LT) vector and untreated (UT) retinas were stained with antibodies against cone  $\alpha$ -transducin (**a**, red) and cone arrestin (**b**, green). (**a**) Restored cone  $\alpha$ -transducin localization to the outer segments of cones in the treated eyes, comparable to wild-type eyes. The images in the first three columns were taken using the same microscope settings, whereas the images in the last column, designated as  $Gucy2e^{-/-}$  UT\*, are identical to those in the  $Gucy2e^{-/-}$  UT column except that they were taken with a long exposure and lighting levels were manipulated in Adobe Photoshop 7.0 Elements to reveal the signal in the red channel. The results indicate substantially reduced levels of cone  $\alpha$ -transducin in untreated  $Gucy2e^{-/-}$  eyes, and restored levels in treated eyes. (**b**) The two left-hand columns are images of retinal sections of eyes harvested and processed under normal light conditions and the right-hand columns are images of those harvested and processed in the dark. In the light, cone arrestin is localized in the cone outer segments and synaptic regions of wild-type as well as treated and untreated  $Gucy2e^{-/-}$  eyes. In the dark, cone arrestin is localized throughout the cone cells in wild-type eyes, and in treated and untreated  $Gucy2e^{-/-}$  eyes. DAPI nuclear counterstain is shown in blue. Scale bars: 15  $\mu$ m. Color images available online at [www.liebertonline.com/hum](http://www.liebertonline.com/hum)

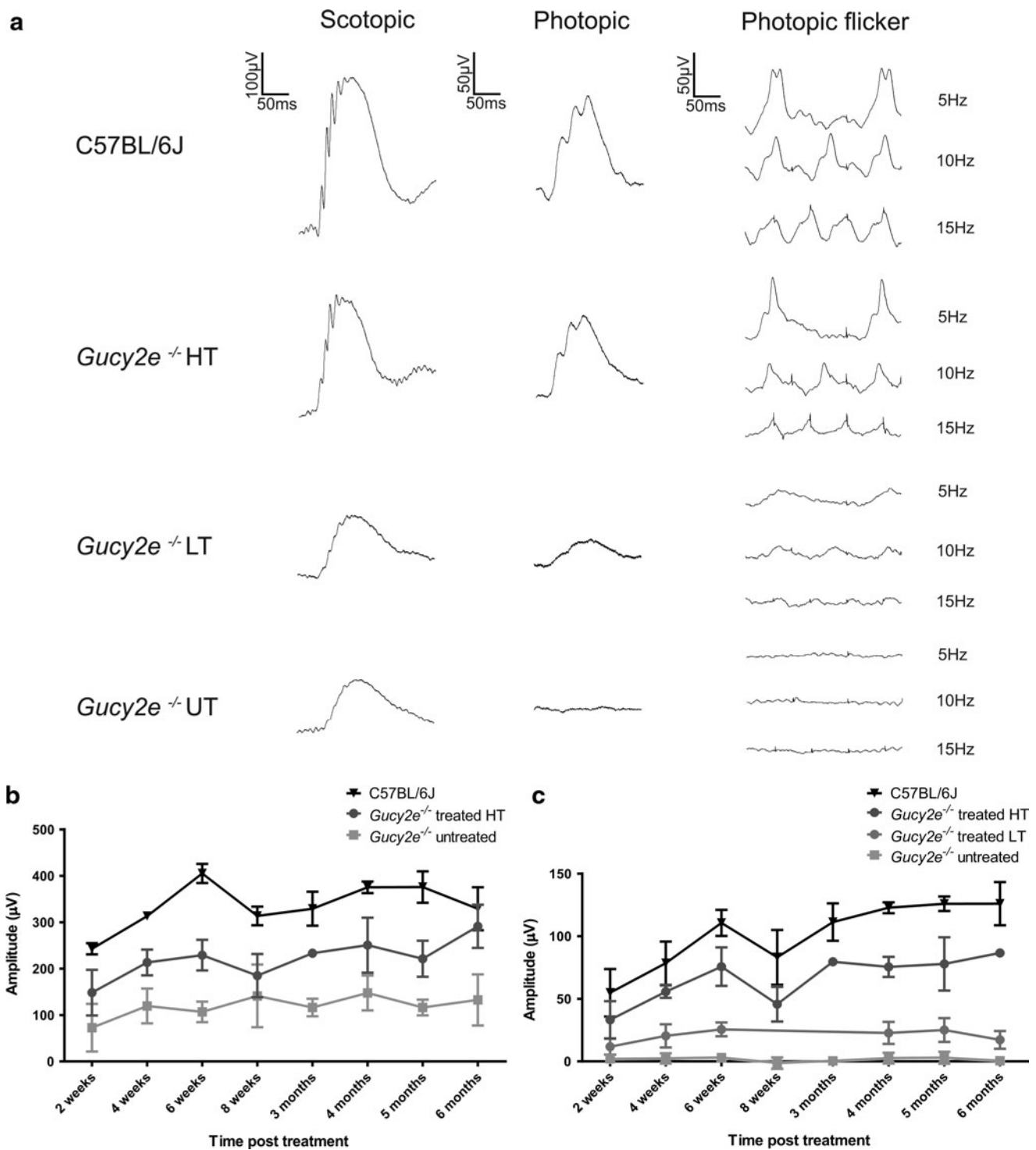


**FIG. 4.** Improvement in cone and rod function in treated *Gucy2e*<sup>-/-</sup> eyes. **(a)** Representative electroretinographic (ERG) traces from C57BL/6J wild-type mice, *Gucy2e*<sup>-/-</sup> mice 6 months after treatment with high-titer (HT) or low-titer (LT) vector, and untreated *Gucy2e*<sup>-/-</sup> (UT) mice. Rod-mediated b-wave responses of *Gucy2e*<sup>-/-</sup> animals treated with low-titer vector were no different from those of untreated eyes, whereas responses of animals treated with high-titer vector were restored to an average of 65% of wild-type amplitudes. Cone-mediated ERG of *Gucy2e*<sup>-/-</sup> animals treated with low-titer vector improved on average to 20% of wild-type amplitudes, whereas the responses of animals treated with high-titer vector were restored to 65% compared with wild-type eyes. **(b)** Over time, scotopic b-wave amplitudes in *Gucy2e*<sup>-/-</sup> mice treated with high-titer vector were significantly higher than those in untreated mice ( $p=0.0005$ , two-way ANOVA). **(c)** Data from animals treated with low-titer vector were significantly different from those of untreated and wild-type eyes at all time points examined ( $p<0.05$ , two-way ANOVA). Cone-mediated ERG responses of eyes treated with high-titer vector were significantly higher than those of untreated eyes at all time points ( $p<0.001$ , two-way ANOVA) and significantly lower than in wild-type eyes at all time points ( $p<0.05$ , two-way ANOVA), except at 2 weeks post injection.

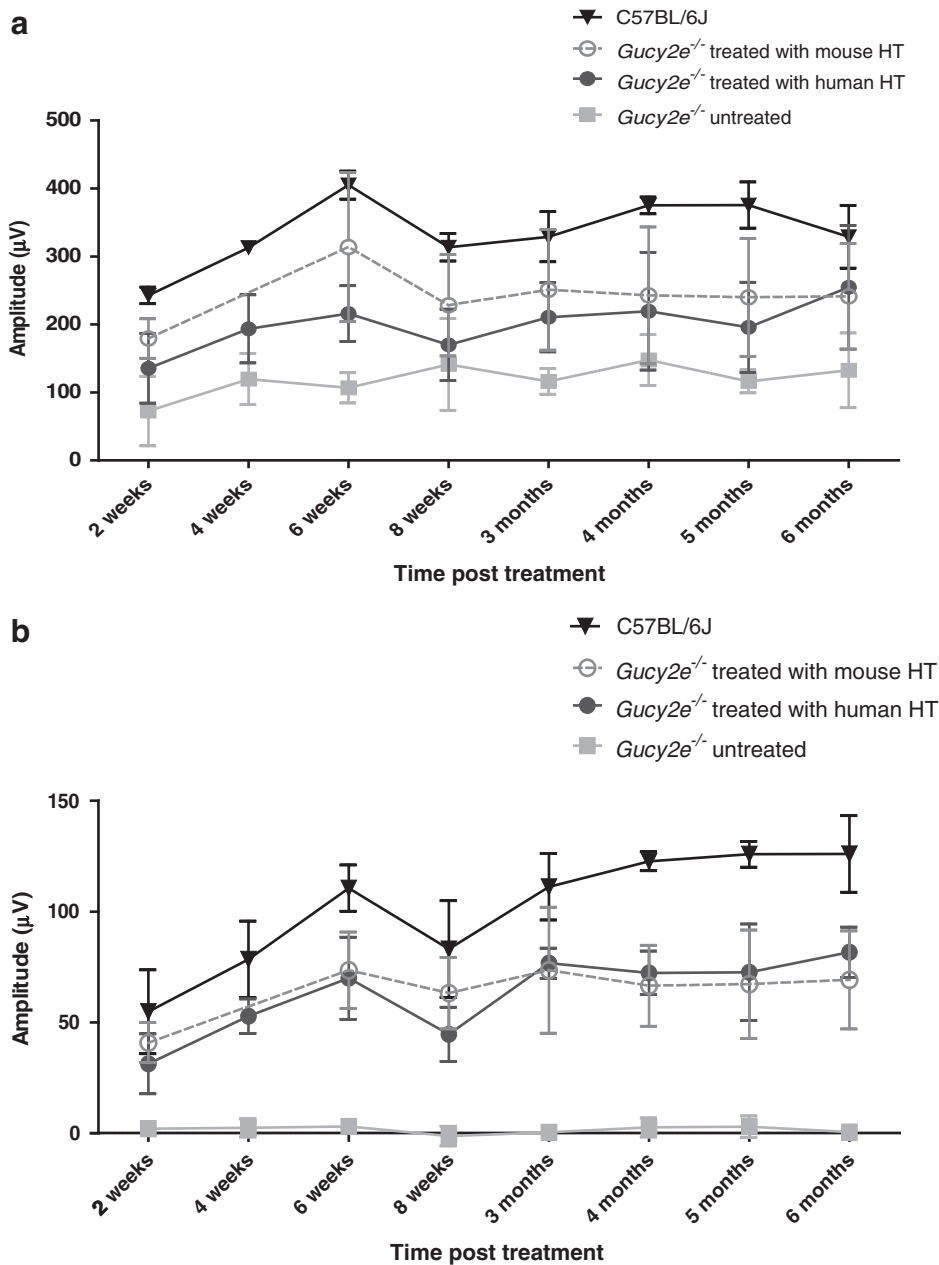


**FIG. 5.** Comparison of photo-receptor function restoration after transfer of human *GUCY2D* and mouse *Gucy2e* transgenes. **(a)** Consistent rod ERG improvement was observed in eyes treated with both vectors (mean  $\pm$  SD). No statistically significant difference was observed between the efficacy of rescue using both vectors ( $p=0.587$ , two-way ANOVA). **(b)** Cone-mediated ERG b-wave responses of *Gucy2e*<sup>-/-</sup> eyes treated with the mouse transcript did not differ from those treated with the human transcript ( $p=0.9887$ , two-way ANOVA). Cone-mediated ERG responses achieved with the mouse transcript were approximately 62% of the response seen in C57BL/6J wild-type eyes, compared with 65% achieved with the human transgene.

#### Improvement in cone-mediated optomotor responses in *Gucy2e*<sup>-/-</sup> mice after treatment

As reported previously (Boye *et al.*, 2010), residual rod function in *Gucy2e*<sup>-/-</sup> animals is sufficient for robust scotopic, rod-mediated optomotor behavior that is equivalent to that in wild-type animals (data not shown). To assess restoration of cone-mediated behavioral responses, optomotor analysis was performed under photopic conditions on *Gucy2e*<sup>-/-</sup> mice 4 months after the animals received subretinal injection of high-titer vector in one eye. We observed a substantial improvement in cone-mediated optokinetic head tracking behavior as a result of treatment (Fig. 6). Cone-mediated visual acuity in untreated *Gucy2e*<sup>-/-</sup> eyes was  $0.102 \pm 0.011$  cycles/degree ( $\pm$ SD,  $n=10$  eyes; Fig. 6a), whereas average visual acuity in

treated eyes was  $0.386 \pm 0.064$  cycles/degree ( $p < 0.0001$ , one-way ANOVA). The visual acuity of treated eyes was significantly lower than that of C57BL/6J wild-type controls, which had an acuity of  $0.518 \pm 0.033$  cycles/degree ( $p < 0.05$ , one-way ANOVA). However, the *Gucy2e*<sup>-/-</sup> mice used for these experiments were of a mixed C57BL6/Sv129 background and the acuity of treated eyes falls within the normal range for other strains of wild-type mice including a mixed C57BL/6J/Sv129 strain ( $0.418 \pm 0.046$  cycles/degree) (Alexander *et al.*, 2007; Haruta *et al.*, 2009; Boye *et al.*, 2010). Contrast sensitivity of treated *Gucy2e*<sup>-/-</sup> eyes improved significantly following treatment ( $1.0 \pm 0.0$  vs.  $5.0 \pm 2.8$ ;  $p < 0.05$ , one-way ANOVA) (Fig. 6b), although it remained significantly lower than the mean contrast sensitivity of C57BL/6J wild-type controls ( $29.3 \pm 5.2$ ;  $p < 0.05$ , one-way ANOVA).

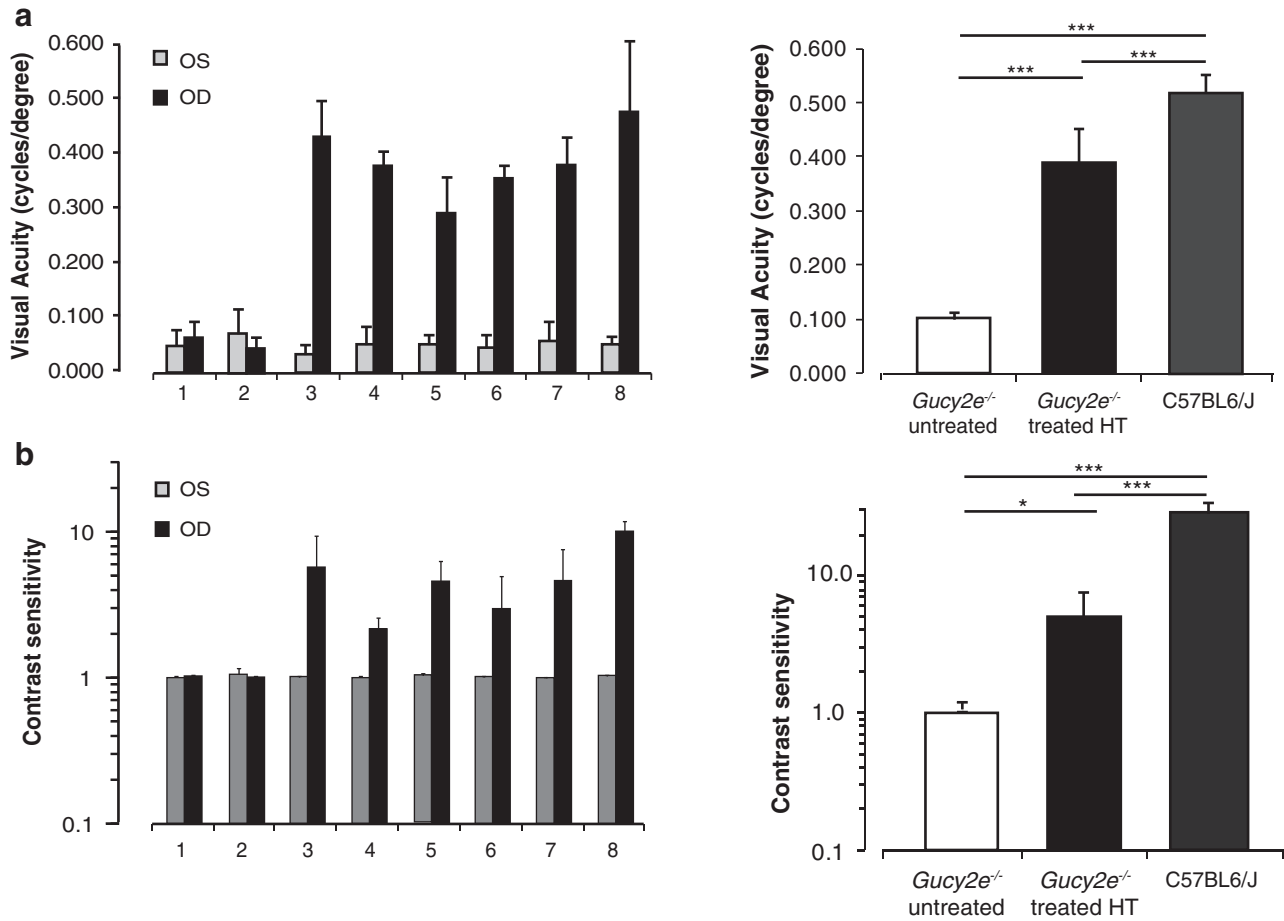


**FIG. 6.** Restoration of cone-mediated optomotor behavior in *Gucy2e*<sup>-/-</sup> treated eyes. Shown is the photopic visual acuity and contrast sensitivity measurements in two untreated *Gucy2e*<sup>-/-</sup> mice (animals 1 and 2), and six mice treated with high-titer vector (animals 3–8) 4 months post treatment. Results are presented for each animal and averaged per group in the right-hand graphs. **(a)** Robust improvement in visual acuity was consistently observed in treated eyes ( $p < 0.0001$ , one-way ANOVA). **(b)** A significant improvement in contrast sensitivity was detected in treated eyes ( $p < 0.05$ , one-way ANOVA). OD, right eye; OS, left eye.

#### Cone preservation in transduced areas of retinas

By using immunolabeling against cone  $\alpha$ -transducin and peanut agglutinin (PNA) lectin, Coleman and colleagues have shown that cone degeneration in *Gucy2e*<sup>-/-</sup> mice starts to be apparent from 9 weeks of age and is slowly progressive (Coleman *et al.*, 2004). Loss of cones is more pronounced in the inferior retina, and by 6 months few cones are present in this region, whereas nearly 50% of cones still remain in the superior retina (Coleman *et al.*, 2004). Because of these regional differences we carried out two subretinal injections in order to administer vector to both superior and inferior retina. Six months after administration of low-titer vector, we analyzed serial sections of treated eyes, using antibodies against cone  $\alpha$ -transducin and GC1 and used age-matched untreated eyes as controls. By staining adjacent sections of the eye we were able to determine whether cone preservation took place in the regions transduced by the vector (Fig. 7). At 6 months posttreatment, both GC1 (green) and cone  $\alpha$ -transducin (yellow) immunostaining were visible in superior and inferior regions of the treated retina, (Fig. 7a, insets e and g; and Fig. 7b, insets f and h). In the areas surrounding

transduced regions, where GC1 immunofluorescence was undetectable (Fig. 7a, insets i and k), no cone  $\alpha$ -transducin staining was seen (Fig. 7b, insets j and l). In untreated *Gucy2e*<sup>-/-</sup> eyes (Fig. 7c, insets m and o), only superior regions of the retina contained cones expressing cone  $\alpha$ -transducin (Fig. 7d, inset n). The staining in these regions was also considerably weaker compared with that in treated retinas. Few cones were detected in the inferior regions of untreated eyes (Fig. 7d, inset p). Quantification of cones in whole eye sections of *Gucy2e*<sup>-/-</sup> eyes treated with low-titer vector and stained with cone  $\alpha$ -transducin revealed a significant overall increase in cone numbers (20%) in treated compared with untreated retinas ( $p < 0.01$ , one-way ANOVA) (Fig. 7r).

By comparing the cone counts described previously with real-time RT-PCR data, we found that there was no statistically significant difference in cone arrestin levels per cone cell between C57BL/6J wild-type ( $26.6 \pm 3.9$  molecules/cone) and untreated *Gucy2e*<sup>-/-</sup> animals ( $19.9 \pm 5.2$  molecules/cone,  $p = 0.1$ , Student *t* test), suggesting that cone arrestin transcript levels are a good indicator of cone numbers. This allowed us to use the previously isolated mRNA samples from the *Gucy2e*<sup>-/-</sup> eyes injected with high-titer vector to determine

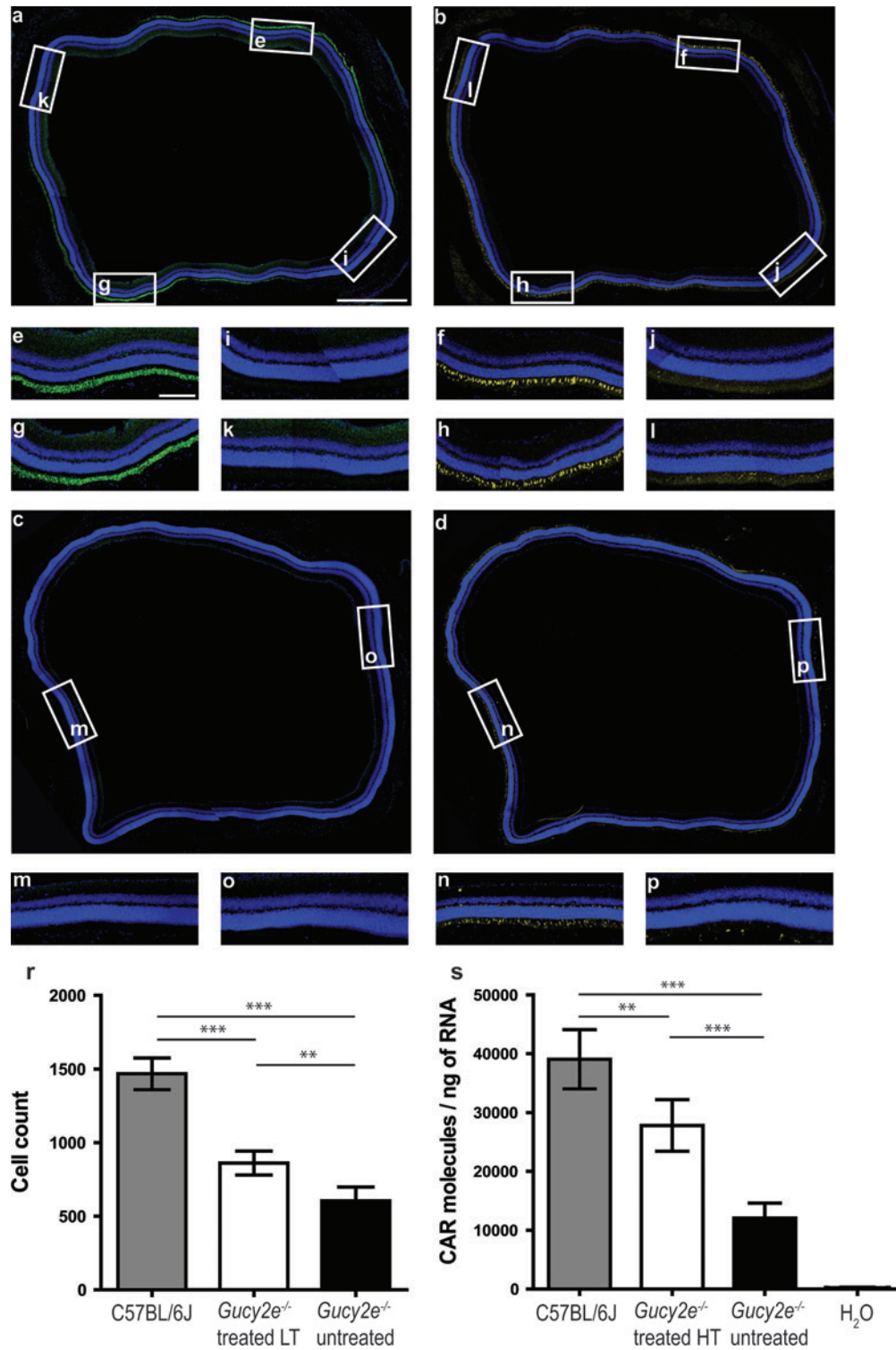


**FIG. 7.** Cone preservation in the transduced areas of *Gucy2e*<sup>-/-</sup> treated eyes. Shown are adjoining retinal sections of *Gucy2e*<sup>-/-</sup> eyes 6 months post treatment with low-titer vector (**a** and **b**) and untreated contralateral eyes (**c** and **d**) stained with antibodies against GC1 (**a** and **c**, green) and cone  $\alpha$ -transducin (**b** and **d**, yellow). (**e**–**l**) *Insets* are images of corresponding regions outlined in (**a**) and (**b**). In the areas where GC1 staining is evident in the treated eyes (**e** and **g**) there is also expression of cone  $\alpha$ -transducin (**f** and **h**). In the untransduced areas, where there is no GC1 (**i** and **k**), there is no cone  $\alpha$ -transducin staining (**j** and **l**). (**m** and **n**) Images of the superior retina, and (**o** and **p**) of the inferior retina of the untreated eye (**c** and **d**). There is no GC1 staining in the inferior part of the retina (**p**). Scale bars: (**a**) 500  $\mu$ m; (**e**) 100  $\mu$ m. (**r**) Number of cone cells determined by cone  $\alpha$ -transducin staining in *Gucy2e*<sup>-/-</sup> eyes treated with low-titer vector, compared with untreated *Gucy2e*<sup>-/-</sup> eyes and C57BL/6J wild-type controls. The cone number in treated eyes was 20% higher than in untreated eyes ( $p < 0.001$ , one-way ANOVA). (**s**) Real-time RT-PCR quantification of cone arrestin mRNA (CAR) in wild-type, *Gucy2e*<sup>-/-</sup> untreated eyes and eyes 5 months post treatment with high-titer vector. The levels of cone arrestin are 1.3 times higher in treated eyes compared with untreated eyes ( $p < 0.0001$ , one-way ANOVA) and have increased to 70% of the levels in wild-type eyes. Color images available online at [www.liebertonline.com/hum](http://www.liebertonline.com/hum)

whether cone preservation was present 6 months post treatment. The levels of cone arrestin mRNA in *Gucy2e*<sup>-/-</sup> eyes treated with high-titer vector were 1.3-fold higher than the arrestin levels in untreated eyes ( $p < 0.0001$ , one-way ANOVA; Fig. 7s). Cone arrestin transcript levels in the treated eyes were restored to 70% of the levels seen in C57BL/6J controls ( $p < 0.001$ , one-way ANOVA).

## Discussion

Gene supplementation studies have been performed in a number of animal models of retinal degeneration, with increasingly encouraging results (Ali *et al.*, 2000; Acland *et al.*, 2001; Pawlyk *et al.*, 2005; Alexander *et al.*, 2007; Tan *et al.*, 2009; Komaromy *et al.*, 2010; Simons *et al.*, 2011). Furthermore, clinical trials have demonstrated the safety and efficacy of AAV2/2-mediated gene therapy for the treatment of LCA2, which is caused by deficiency in *RPE65* (Bainbridge *et al.*, 2008; Hauswirth *et al.*, 2008; Maguire *et al.*, 2008).

In this study we assessed the efficacy of an rAAV2/8 vector carrying a human *GUCY2D* transgene in the *Gucy2e*<sup>-/-</sup> model of LCA1. It follows two previous studies in which AAV2/5 vectors carrying either the bovine or mouse GC1 transgene were used to treat the *Gucy2e*<sup>-/-</sup> mouse (Haire *et al.*, 2006; Boye *et al.*, 2010). Use of the bovine transgene did not improve retinal function (Haire *et al.*, 2006). Although use of an rAAV2/5 vector carrying the mouse transgene resulted in significant improvements in cone ERGs (photopic b-wave amplitudes up to 45% of wild type), and also in cone-mediated vision, no improvements were seen in rod ERGs (Boye *et al.*, 2010). Although cone preservation was demonstrated, the assessments were made at 3 to 4 months of age, at a time when cones are still plentiful in the superior regions and degenerating in inferior retinas.

In this study we used an rAAV2/8 serotype as previously we and other groups have demonstrated more efficient transduction of photoreceptor cells as well as higher levels of transgene expression after the use of this serotype compared with AAV2/5 (Yang *et al.*, 2002; Allogica *et al.*, 2007; Natkunarajah *et al.*, 2008). After administration of the vector, we achieved the most successful rescue of the *Gucy2e*<sup>-/-</sup> mouse model to date. We demonstrated appropriate localization of the GC1 transgene product to the outer segments of rods and cones and increased levels and appropriate localization of cone  $\alpha$ -transducin. In addition to the restoration of cone ERG function to near wild-type levels and a robust improvement in cone-mediated visual function, we also demonstrated for the first time a significant improvement in rod ERG function and long-term preservation of cones.

A study of adult patients with LCA1 ranging in age from 20 to 53 years has reported preservation of retinal structures despite markedly impaired visual acuity (Pasadhika *et al.*, 2010). This suggests that LCA1 is a fairly stationary condition with minor structural deterioration with age, and that there might be a relatively long opportunity for treatment compared, for instance, with patients of a similar age with *RPE65* mutations whose retinal structures are compromised to a greater extent (Pasadhika *et al.*, 2010). Thus vectors similar to the one used in this study could be suitable for use in a clinical trial and have the potential to be highly effective in patients with LCA1.

## Acknowledgments

The authors thank Professor David Garbers for providing the *Gucy2e*<sup>-/-</sup> mouse line, Professor Alexander Dizhoor for providing the GC1 antibody used for immunostaining, as well as Mark Basche for help with virus purification. This work was supported by grants from the Medical Research Council, European Union AAVEYE, and the British Retinitis Pigmentosa Society. R.R.A. and J.W.B. are supported by the NIHR Biomedical Centre for Ophthalmology at Moorfields Eye Hospital. R.A.P. is a Royal Society University Research Fellow (RG080398). Funding to pay the Open Access publication charges for this paper was provided by the Wellcome Trust (grant no. 082217).

## Author Disclosure Statement

No competing financial interests exist for any of the authors.

## References

- Acland, G.M., Aguirre, G.D., Ray, J., *et al.* (2001). Gene therapy restores vision in a canine model of childhood blindness. *Nat. Genet.* 28, 92–95.
- Alexander, J.J., Umino, Y., Everhart, D., *et al.* (2007). Restoration of cone vision in a mouse model of achromatopsia. *Nat. Med.* 13, 685–687.
- Ali, R.R., Sarra, G.M., Stephens, C., *et al.* (2000). Restoration of photoreceptor ultrastructure and function in retinal degeneration slow mice by gene therapy. *Nat. Genet.* 25, 306–310.
- Allogica, M., Mussolino, C., Garcia-Hoyos, M., *et al.* (2007). Novel adeno-associated virus serotypes efficiently transduce murine photoreceptors. *J. Virol.* 81, 11372–11380.
- Baehr, W., Karan, S., Maeda, T., *et al.* (2007). The function of guanylate cyclase 1 and guanylate cyclase 2 in rod and cone photoreceptors. *J. Biol. Chem.* 282, 8837–8847.
- Bainbridge, J.W., Smith, A.J., Barker, S.S., *et al.* (2008). Effect of gene therapy on visual function in Leber's congenital amaurosis. *N. Engl. J. Med.* 358, 2231–2239.
- Boye, S.E., Boye, S.L., Pang, J., *et al.* (2010). Functional and behavioral restoration of vision by gene therapy in the guanylate cyclase-1 (GC1) knockout mouse. *PLoS One* 5, e11306.
- Coleman, J.E., and Semple-Rowland, S.L. (2005). GC1 deletion prevents light-dependent arrestin translocation in mouse cone photoreceptor cells. *Invest. Ophthalmol. Vis. Sci.* 46, 12–6.
- Coleman, J.E., Zhang, Y., Brown, G.A., and Semple-Rowland, S.L. (2004). Cone cell survival and downregulation of GCAP1 protein in the retinas of GC1 knockout mice. *Invest. Ophthalmol. Vis. Sci.* 45, 3397–3403.
- Davidoff, A.M., Ng, C.Y., Sleep, S., *et al.* (2004). Purification of recombinant adeno-associated virus type 8 vectors by ion exchange chromatography generates clinical grade vector stock. *J. Virol. Methods* 121, 209–215.
- den Hollander, A.I., Roepman, R., Koenekoop, R.K., and Cremers, F.P. (2008). Leber congenital amaurosis: Genes, proteins and disease mechanisms. *Prog. Retin. Eye Res.* 27, 391–419.
- Douglas, R.M., Alam, N.M., Silver, B.D., *et al.* (2005). Independent visual threshold measurements in the two eyes of freely moving rats and mice using a virtual-reality optokinetic system. *Vis. Neurosci.* 22, 677–684.
- Elias, R.V., Sezate, S.S., Cao, W., and McGinnis, J.F. (2004). Temporal kinetics of the light/dark translocation and compartmentation of arrestin and  $\alpha$ -transducin in mouse photoreceptor cells. *Mol. Vis.* 10, 672–681.

- Gao, G.P., Alvira, M.R., Wang, L., *et al.* (2002). Novel adeno-associated viruses from rhesus monkeys as vectors for human gene therapy. *Proc. Natl. Acad. Sci. U.S.A.* 99, 11854–11859.
- Haire, S.E., Pang, J., Boye, S.L., *et al.* (2006). Light-driven cone arrestin translocation in cones of postnatal guanylate cyclase-1 knockout mouse retina treated with AAV-GC1. *Invest. Ophthalmol. Vis. Sci.* 47, 3745–3753.
- Hanein, S., Perrault, I., Gerber, S., *et al.* (2004). Leber congenital amaurosis: Comprehensive survey of the genetic heterogeneity, refinement of the clinical definition, and genotype–phenotype correlations as a strategy for molecular diagnosis. *Hum. Mutat.* 23, 306–317.
- Haruta, M., Bush, R.A., Kjellstrom, S., *et al.* (2009). Depleting Rac1 in mouse rod photoreceptors protects them from photo-oxidative stress without affecting their structure or function. *Proc. Natl. Acad. Sci. U.S.A.* 106, 9397–9402.
- Hauswirth, W.W., Aleman, T.S., Kaushal, S., *et al.* (2008). Treatment of Leber congenital amaurosis due to *RPE65* mutations by ocular subretinal injection of adeno-associated virus gene vector: Short-term results of a phase I trial. *Hum. Gene Ther.* 19, 979–990.
- Helten, A., Saftel, W., and Koch, K.W. (2007). Expression level and activity profile of membrane bound guanylate cyclase type 2 in rod outer segments. *J. Neurochem.* 103, 1439–1446.
- Hunt, D.M., Buch, P., and Michaelides, M. (2010). Guanylate cyclases and associated activator proteins in retinal disease. *Mol. Cell. Biochem.* 334, 157–168.
- Khani, S.C., Pawlyk, B.S., Bulgakov, O.V., *et al.* (2007). AAV-mediated expression targeting of rod and cone photoreceptors with a human rhodopsin kinase promoter. *Invest. Ophthalmol. Vis. Sci.* 48, 3954–3961.
- Koch, K.W., Duda, T., and Sharma, R.K. (2002). Photoreceptor specific guanylate cyclases in vertebrate phototransduction. *Mol. Cell. Biochem.* 230, 97–106.
- Komaromy, A.M., Alexander, J.J., Rowlan, J.S., *et al.* (2010). Gene therapy rescues cone function in congenital achromatopsia. *Hum. Mol. Genet.* 19, 2581–2593.
- Larhammar, D., Nordstrom, K., and Larsson, T.A. (2009). Evolution of vertebrate rod and cone phototransduction genes. *Philos. Trans. R. Soc. Lond. B Biol. Sci.* 364, 2867–2880.
- Lobanova, E.S., Herrmann, R., Finkelstein, S., *et al.* (2010). Mechanistic basis for the failure of cone transducin to translocate: Why cones are never blinded by light. *J. Neurosci.* 30, 6815–6824.
- Maguire, A.M., Simonelli, F., Pierce, E.A., *et al.* (2008). Safety and efficacy of gene transfer for Leber's congenital amaurosis. *N. Engl. J. Med.* 358, 2240–2248.
- Natkunaratnam, M., Tritsch, P., McIntosh, J., *et al.* (2008). Assessment of ocular transduction using single-stranded and self-complementary recombinant adeno-associated virus serotype 2/8. *Gene Ther.* 15, 463–467.
- Pasadhika, S., Fishman, G.A., Stone, E.M., *et al.* (2010). Differential macular morphology in patients with *RPE65*-, *CEP290*-, *GUCY2D*-, and *AIPL1*-related Leber congenital amaurosis. *Invest. Ophthalmol. Vis. Sci.* 51, 2608–2614.
- Pawlyk, B.S., Smith, A.J., Buch, P.K., *et al.* (2005). Gene replacement therapy rescues photoreceptor degeneration in a murine model of Leber congenital amaurosis lacking RPGRIP. *Invest. Ophthalmol. Vis. Sci.* 46, 3039–3045.
- Pawlyk, B.S., Bulgakov, O.V., Liu, X., *et al.* (2010). Replacement gene therapy with a human RPGRIP1 sequence slows photoreceptor degeneration in a murine model of Leber congenital amaurosis. *Hum. Gene Ther.* 21, 993–1004.
- Simons, D.L., Boye, S.L., Hauswirth, W.W., and Wu, S.M. (2011). Gene therapy prevents photoreceptor death and preserves retinal function in a Bardet-Biedl syndrome mouse model. *Proc. Natl. Acad. Sci. U.S.A.* 108, 6276–6281.
- Sun, X., Pawlyk, B., Xu, X., *et al.* (2010). Gene therapy with a promoter targeting both rods and cones rescues retinal degeneration caused by *AIPL1* mutations. *Gene Ther.* 17, 117–131.
- Tan, M.H., Smith, A.J., Pawlyk, B., *et al.* (2009). Gene therapy for retinitis pigmentosa and Leber congenital amaurosis caused by defects in *AIPL1*: Effective rescue of mouse models of partial and complete *Aipl1* deficiency using AAV2/2 and AAV2/8 vectors. *Hum. Mol. Genet.* 18, 2099–2114.
- Williams, M.L., Coleman, J.E., Haire, S.E., *et al.* (2006). Lentiviral expression of retinal guanylate cyclase-1 (*RetGC1*) restores vision in an avian model of childhood blindness. *PLoS Med.* 3, e201.
- Yang, G.S., Schmidt, M., Yan, Z., *et al.* (2002). Virus-mediated transduction of murine retina with adeno-associated virus: Effects of viral capsid and genome size. *J. Virol.* 76, 7651–7660.

Address correspondence to:  
 Dr. Robin R. Ali  
 Department of Genetics  
 University College London  
 UCL Institute of Ophthalmology  
 London EC1V 9EL  
 United Kingdom

E-mail: r.ali@ucl.ac.uk

Received for publication April 22, 2011;  
 accepted after revision June 13, 2011.

Published online: June 14, 2011.